IEEE Access
Multidisciplinary : Rapid Review : Open Access Journal

Received August 5, 2021, accepted August 31, 2021, date of publication September 3, 2021, date of current version September 17, 2021.

Digital Object Identifier 10.1109/ACCESS.2021.3110431

Design and Control of Grid-Connected PWM Rectifiers by Optimizing Fractional Order PI Controller Using Water Cycle Algorithm

SUSHMA KAKKAR[1], TANMOY MAITY[1], (Member, IEEE), RAJESH KUMAR AHUJA[2], (Member, IEEE), PRATIMA WALDE[3], R. K. SAKET[3], (Senior Member, IEEE), BASEEM KHAN[4], (Member, IEEE), AND SANJEEVIKUMAR PADMANABAN[5], (Senior Member, IEEE)

[1]Department of Mining Machinery Engineering, Indian Institute of Technology (Indian School of Mines), Dhanbad 826004, India
[2]Electrical Engineering Department, J. C. Bose University of Science and Technology, YMCA, Faridabad 121006, India
[3]Department of Electrical Engineering, Indian Institute of Technology (BHU), Varanasi, Uttar Pradesh 221005, India
[4]Department of Electrical Engineering, Hawassa University, Hawassa 05, Ethiopia
[5]CTiF Global Capsule, Department of Business Development and Technology, Aarhus University, 7400 Herning, Denmark

Corresponding authors: Baseem Khan (baseem.khan04@gmail.com) and R. K. Saket (rksaket@ieee.org)

ABSTRACT In this paper water cycle algorithm-based fractional order PI controller (FOPI) is proposed for virtual flux-oriented control of a three-phase grid-connected PWM rectifier. FOPI controller makes the PWM rectifier control more robust due to the fractional behavior. Fractional-order controllers have an additional degree of freedom, so a wider range of parameters is available to provide better control and robustness in the plant. The optimization and design of the FOPI controller are done using the water cycle algorithm (WCA). WCA is an optimization method inspired by monitoring the water cycle operation and flow of water bodies like streams and rivers toward the sea. The performance of the FOPI controller is compared with the classical integer order PI controller. The parameters of PI and FOPI controllers are optimized and designed using the WCA technique, leading to WCA-PI and WCA-FOPI controllers. The system is tested using MATLAB/Simulink. The simulation results verify the better performance of WCA-FOPI in terms of settling time, rise time, peak overshoot, and Total Harmonic Distortion (THD) of grid current. A robustness measurement with line filter parametric variations and non-ideal supply voltage (unbalance and distorted supply voltage) is carried out. The WCA-FOPI demonstrates more robustness as compared to WCA-PI. Simulation findings validate the WCA-FOPI controller outcomes as compared to WCA-PI in terms of control effect and robustness.

INDEX TERMS PWM rectifier, VFOC, water cycle algorithm, FOPID controller, fractional calculus.

I. INTRODUCTION

The power electronics converters are being used at all levels in power systems using renewable energy sources. The most used power converter topology is the three-phase voltage source converter. This converter is popular due to its capability to operate either as a rectifier or inverter. In rectifier mode, it is more commonly called a PWM rectifier. PWM rectifiers have been an ideal choice among different power quality improved rectifiers. The attractive features of these rectifiers are better control of dc voltage, nearly unity power factor operation (grid voltage and current in the same phase), and less harmonic content in grid current. The researchers feel the need for advanced control techniques of active rectifiers. One popular control method known as voltage-oriented control (VOC) indirectly provides active and reactive power control. Although VOC provides a satisfactory response, the operation is largely affected by the chosen current controller [1]. In the VOC method, the ac side currents are transformed into active and reactive components and compared with reference currents. The PI controllers are used to track the reference. Modulator block is used to generate gate signals. Fine-tuning of PI controller is necessary to get a satisfactory steady and dynamic response.

The associate editor coordinating the review of this manuscript and approving it for publication was Suman Maiti.

Another method that is simple to implement is known as the direct power control (DPC) method. In this method, the active and reactive power is brought near reference values without using inner current control loops. Therefore, the co-ordinate transformations are not needed [2]. The error in powers (active and reactive), hysteresis controller, and a switching logic table are used to produce the PWM signals. Therefore, no modulating blocks are required in DPC. So, the performance of DPC depends on the accurate calculation or measurement of active and reactive power [2]. However, hysteresis regulators ensure good dynamic behavior, but the drawback with DPC is not getting constant switching frequency. Another downside is the requirement of high sampling frequency. The behavior of hysteresis regulators used in DPC causes the variable switching pattern of the semiconductor devices used in the converter [3]. The space vector pulse width modulation technique can obtain constant switching frequency with DPC [1], [4]. The VOC and DPC methods can be applied based on voltage estimation using virtual flux and are called virtual flux-based VOC (VFOC) and virtual flux-based DPC (VFDPC) methods.

PID controllers are well known for control applications in the industry due to their simple configuration. However, to get high performance, tuning is necessary [5]. The unfolding of fractional calculus has shown the way towards changeover from classical PID controllers to fractional order PID (FOPID) controllers. The differential equations are of non-integer order in FOPID. A comparison of integer order and fractional order controllers is made for real-life objects. In industrial problems, the fractional-order controllers are found better and require less control effort than integer-order controllers [6]. The author has explained the benefits, execution, and commercial uses of FOPID controllers.

The changeover from integer-order controllers to fractional-order controllers can be implemented globally. It can provide more tuning flexibility and better design specifications. The future focus should be to evolve the tools and directions to implement the transition to FOPID controllers [7]. The author has used FOPID in a hybrid renewable power plant for integration through a voltage source inverter. The power quality of the injected power is improved as compared to classical PID controller. The fractional-order controller is less sensitive to variations in load and parameters, which means more freedom in choosing controller parameters. This allows us to pick out economic electronic components for the plant [8]. FOPID is used for grid integrated PV systems to inject active and reactive power individually. The power quality of injected power is improved using the FOPI controller during irradiation and load changes [9]. FOPID controller is used for stability control in a magnetic levitation system. The Maglev system model is designed in MATLAB/Simulink using the first principle, which can be used for other applications. The fractional-order controller demonstrated an extremely better response compared to the integer-order controller [10]. The author has used the FOPID controller in a hybrid shunt active power filter to compensate for harmonics and reactive power. The system is implemented under unbalance supply and with unbalanced load conditions. The developed system is economical, not complex, easy to implement, and effectively eliminates the harmonics load [11]. A FOPID controller is designed for a DC-DC boost converter under different operating conditions. The simulation and experimental results show better overshoot and recovery time using the fractional-order controller than the integer-order controller. The author suggested that fractional-order controllers can be applied in step-down and buck-boost DC-DC converters using the same formulations [12]. FOPID controller is applied to three-phase induction motors to reduce the harmonic current, vibration, and noise. The controller design is based on the motor parameters [13]. A FOPID based on fuzzy is used in automatic governor control and tuned using the imperialist competitive method. The simulation is implemented for isolated and interconnected systems. The FOPID controller is compared with other existing controllers. The system with FOPID is robust against parameters and load variations [14].

As classical PID controllers need tuning of parameters, the same applies to FOPID controllers as well. Several tuning methods can be found in the literature to tune the parameters of PID controllers [15]. To achieve optimal tuning, meta-heuristic methods prove to be better than trial and error-based approaches and Zigler-Nichol's methods. A cuckoo search algorithm is used in [16] to tune the PID controller parameters of an AVR system to improve the response. The simulation results validate better control action of cuckoo search (CS) algorithm compared to particle swarm optimization (PSO) and artificial bee colony (ABC) method. The kidney-inspired method is used in [17] to tune the PID controller parameters of an AVR system to improve the transient response. The peak overshoot, rise time, settling time are reduced, and steady-state error is eliminated. The optimization methods used for PID controllers can also be used to tune the parameters of FOPID controllers. FOPID controllers offer much better adaptive behavior due to their five parameters available for tuning. The tuning algorithm for FOPID controllers is reviewed in [7]. The different methods have been applied for tuning of FOPID controller parameters in the literature, such as simulated annealing, genetic algorithm, chaotic ant swarm, grey wolf optimization, particle swarm optimization, slap swarm algorithm, colliding bodies optimization, tabu search-based algorithm, continuous state transition, moth flame, fire-fly and other meta-heuristic algorithms [7]. FOPID controllers are applied to AVR systems in many research papers, and different optimization techniques have been used to tune the controller parameters. A chaotic ant swarm (CAS) algorithm is used to tune the parameters of the FOPID controller in an AVR system. The objective function is to improve the transient response and reduce the steady-state error. The simulation results verify the better performance of the CAS-FOPID controller under model uncertainties also [18]. The author has used the FOPID controller for AVR in [19] to improve multi-objective functions.

The three objectives optimized are integral of absolute error (IAE), absolute steady-state error, and settling time. A multi-objective external optimization (MOEO) technique is proposed to achieve multi-objective optimization. The Simulated Annealing (SA) method is used in an AVR system to tune the parameters of the FOPID controller. The cost function is minimized using the SA method. The results indicated good control action and robustness against model uncertainties [20]. The employment of fraction calculus in the power system has been studied in voltage control, automatic governor control, and damping control [21]. The prospects of FOPID controllers in power converter applications are not explored until recently.

This paper proposes a water cycle algorithm-based fractional order PI controller (FOPI) for virtual flux-oriented control of a three-phase grid-connected PWM rectifier. FOPI controller makes the PWM rectifier control more robust due to the fractional behavior. Fractional-order controllers have an additional degree of freedom, and so a wider region of parameters is available to provide better control and robustness in the plant. One FOPI controller is used in the outer voltage loop and two FOPI current controllers in the inner current loops. The classical PI controllers are also used for comparison purpose. The optimization and design of both PI and FOPI controller is done using water cycle algorithm (WCA) technique leading to WCA-PI and WCA-FOPI controllers. The simulation results verify the better performance of WCA-FOPI in terms of less settling time, rise time, peak overshoot, and Total Harmonic Distortion (THD) of grid current. A robustness measurement with parametric filter variations and non-ideal supply voltage (unbalance and distorted supply voltage) is carried out. The WCA-FOPI demonstrates more robustness as compared to WCA-PI. Simulation findings validate the WCA-FOPI controller outcomes as compared to WCA-PI in terms of control effect and robustness.

The highlights of the current work are to:

- Develop a Simulink model of a VFOC based PWM rectifier.
- Design and optimize the WCA-PI controller for inner and outer loop controls.
- Design and optimize the WCA-FOPI controller for inner and outer loop controls.
- Estimate and compare the control actions of WCA-PI and WCA-FOPI controllers under balanced supply voltage conditions.
- Estimate and compare the control actions of WCA-PI and WCA-FOPI controllers under parametric variations.
- Estimate and compare the control actions of WCA-PI and WCA-FOPI controllers under unbalanced and distorted supply voltage conditions.

This research paper is divided into eight parts. The model of the rectifier and VFOC algorithm is explained in part II. The fractional-order PID controller is discussed in part III. Part IV presents the water cycle algorithm. Part V presents the MATLAB simulation results, and part VI deals with the conclusion.

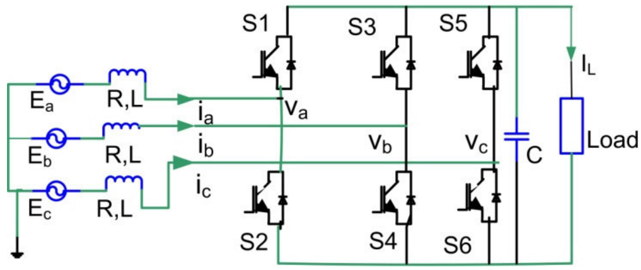

FIGURE 1. PWM Rectifier.

II. PWM RECTIFIER AND VFOC ALGORITHM

The three-phase PWM rectifier circuit is shown in Fig.1.Six IGBT switches have been used in the bridge configuration. The line filter with resistance R and inductance L is connected on the input side. The line currents are labeled as i_a, i_b, i_c and the three phase ac voltages as E_a, E_b, E_c. The DC side of the converter is represented by of a filter C and a load resistance R_L. The load voltage and current are V_{dc} and I_L, respectively. S_a, S_b and S_c are the switching state of the converter.

Applying the Kirchhoff's voltage law in Fig.1:

$$\begin{bmatrix} E_a \\ E_b \\ E_c \end{bmatrix} = R\begin{bmatrix} i_a \\ i_b \\ i_c \end{bmatrix} + L\frac{d}{dt}\begin{bmatrix} i_a \\ i_b \\ i_c \end{bmatrix} + \begin{bmatrix} v_a \\ v_b \\ v_c \end{bmatrix} \tag{1}$$

$$\frac{dv_c}{dt} = S_a i_a + S_b i_b + S_c i_c \tag{2}$$

The pole phase voltage of the rectifier is represented by the equation (3) to (5):

$$v_{an} = (2S_a - (S_b + S_c))\frac{V_{dc}}{3} \tag{3}$$

$$v_{bn} = (2S_b - (S_a + S_c))\frac{V_{dc}}{3} \tag{4}$$

$$v_{cn} = (2S_c - (S_a + S_b))\frac{V_{dc}}{3} \tag{5}$$

The co-ordinates transformation from three phases (abc) to stationary co-ordinates (α-β) is done using the following equation.

$$\begin{bmatrix} x_\alpha \\ x_\beta \end{bmatrix} = \frac{2}{3}\begin{bmatrix} 1 & -1/2 & -1/2 \\ 0 & \sqrt{3}/2 & \sqrt{3}/2 \end{bmatrix}\begin{bmatrix} x_a \\ x_b \\ x_c \end{bmatrix} \tag{6}$$

The VFOC algorithm based on voltage-oriented control without ac line voltage sensor is applied. The voltage is estimated as in [3]. The FOPI controllers are used in place of traditional PI controllers in the inner current loop and outer voltage loop. The parameters of FOPID controllers are optimized and designed using water cycle algorithm.

III. FRACTION ORDER PID CONTROLLER

In recent times, fraction order calculus has gained attention, and applications have been explored in the field of control

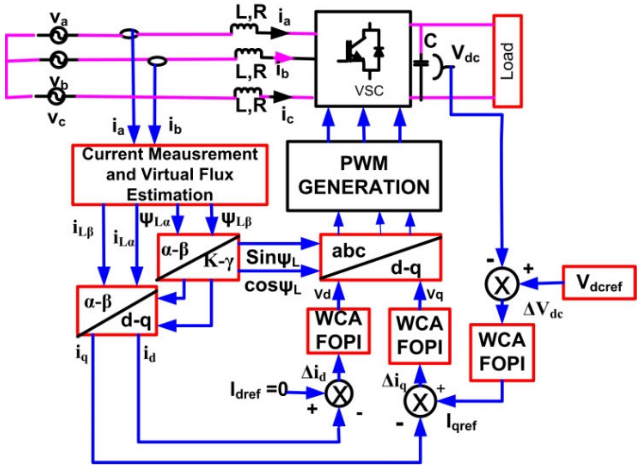

FIGURE 2. VFOC Scheme using WCA optimized FOPI controllers.

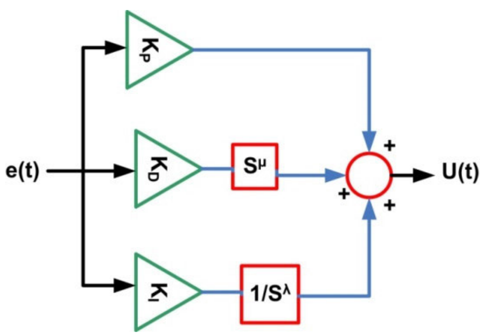

FIGURE 3. FOPID Controller.

system [22]–[24]. Fractional order calculus can represent better, and accurate model of real system as compared to classical integer theory.

The analysis of fractional order differential equations is given in [25], [26]. The study on FOPID controllers is focused on the academic and commercial fields. The benefits of FOPID controllers are moreover attractive in electrical, mechanical, and electromechanical system models exhibiting characteristics of real materials and theological features of rocks and more. The derivative and integral order is an integer in classical PID controller, whereas in FOPID controller, they are fractional.

Podlunby put forward the idea of FOPID in year 1997. Podlunby found that FOPID controllers can perform better than PID controllers. The structure of FOPID is represented by $PI^{\lambda}D^{\mu}$ in [23], [24]. The λ and μ are fraction numbers. The Fig.3 illustrates the schematic of FOPID controller.

The control action of FOPID controller can be represented equation (7):

$$u(t) = K_p e(t) + K_i D^{-\lambda} e(t) + K_d D^{\mu} e(t) \tag{7}$$

The λ and μ are random real numbers. In case of a classical PID controller, these values are equal to one.

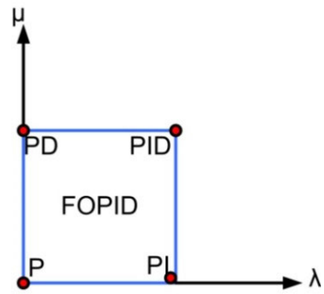

FIGURE 4. FOPID and PID Controller domain.

The equation (7) can be written in the s-domain as:

$$u(s) = \left(K_p + \frac{K_i}{S^{\lambda}} + K_E S^{\mu}\right) e(s) \tag{8}$$

The control domain of PID and FOPID can be shown in Fig.4.

The major benefit of the FOPID controller is to increase in performance of non-linear and dynamic systems and have less sensitivity to changes in parameters of the system. However, the challenges involved are the design and implementation costs. The FOPID controller requires five parameters, whereas the PID controller needs to optimize only three parameters. Hence, the design of the FOPID controller is more challenging than the PID controller. Although more technically helpful, the implementation cost and cost benefits obtained from the FOPID controller need further investigation. The prospects of FOPID controllers in power converter applications are not explored until recently. The employment of fraction calculus in power systems has been studied in the areas of voltage control, automatic governor control and damping control.

The design and tuning of controller parameters are very crucial part in a control system. Usually the trial-and-error procedure is used to tune the parameters of a PID controller. The controller parameters obtained by this method are time-consuming and may not be the finest ones. Optimization techniques are sought after as they require less time and give optimal parameter values [27]. Particle swarm optimization (PSO) is used in [28]–[30] to tune the fractional-order controllers. Atom search optimization (ASO) method is used for tuning of FOPID controller and to control the frequency automatically in a hybrid power system [31]. The ASO method is quite simple to apply and based on the theory of atomic motion behavior and can be used in to find optimal solutions in broad range of applications. An advanced design of ASO method is ChASO. This method is established based on logistic map chaotic pattern, and a better solution is obtained by avoiding local minima stagnancy. The author uses the ChASO in [32] to control the speed of dc motor. Adaptive Colliding Bodies Optimization (ACBO) method has been used for tuning of FOPID in [27] for robotic control. Some others optimization techniques such as Tabu search, harmony search, grey wolf optimization, Quantum bacterial foraging have been used in literature [33]–[36].

IV. WATER CYCLE ALGORITHM

Water cycle algorithm (WCA) is based on imitation of nature inspired water cycle process and describes how the water flow from high mountain ranges through rivers, streams, and merges into sea. The rainwater is collected in streams and rivers and finds way towards the sea. This water is converted into vapors and cause cloud formation. The clouds on condensation let out the water back by means of rain drops or snowfall and get collected in streams and rivers. The WCA follows the water cycle approach by irregularly created rain drops. The raindrops can be characterized by an array and leads to the optimal solution of a problem. The sea is called the lowest point as the water finally gets collected into the sea through rivers and streams. The sea or rivers or streams are considered as rain drops by this algorithm. Where sea is the finest rain drop, as it has least objective function value (for minimization). Thereafter, rivers having values nearest to the best objective value are chosen. Rivers proceed on the way to sea and streams proceed towards rivers or move to sea. The water cycle algorithm finds new solution as water move to the sea. The rivers move towards sea and vaporization of sea water takes place. If all rivers approach the same fitness values as sea, it means complete vaporization has happened. So, the rain starts again and hence completion of the water cycle. If a stream moving into a river discovers a better value of cost function, then the direction of flow is reversed (position of stream and river is interchanged).

A stream is specified by a matrix A as below:

$$A_i = [A_1 A_2 A_3 A_4 \ldots.., A_N] \tag{9}$$

Suppose the total number of streams is considered of size Npop. In that case, the whole population consisting of sea plus rivers can be expressed by an arbitrarily formed matrix of dimensions $N_{POP} \times$ N as below:

$$Total\ Population = \begin{bmatrix} Sea \\ R_1 \\ R_2 \\ R_3 \\ . \\ . \\ . \\ S_{Nsr+1} \\ S_{Nsr+2} \\ S_{Nsr+3} \\ . \\ . \\ S_{N_{POP}} \end{bmatrix} = \begin{bmatrix} A_1^1 & A_2^1 & A_3^1 & \ldots & A_N^1 \\ A_1^2 & A_2^2 & A_3^2 & \ldots & A_N^2 \\ . & . & . & . & . \\ . & . & . & . & . \\ A_1^{N_{POP}} & A_2^{N_{POP}} & A_3^{N_{POP}} & . & A_N^{N_{POP}} \end{bmatrix} \tag{10}$$

The N_{POP} is the population size and N is the design variable. The defined, designed variables in the matrix can be real values (floating type). Considering the cost function, the cost of every stream (each row is a stream) can be found below.

$$C_i = Cost_i = f\left(A_1^i, A_2^i, \ldots\ldots., A_N^i\right) \quad i = 1, 2, 3, \ldots\ldots, N_{POP} \tag{11}$$

The best stream (which has the least cost or most fitness) is picked as the rivers and sea. The best stream is recognized as the sea. So, Nsr is the sum of the number of rivers and one sea. The remaining population i.e., N_{stream} is recognized as streams moving to rivers or merging straight into the sea. The following equations can represent this:

$$N_{sr} = Number\ of\ rivers + 1\ (sea) \tag{12}$$

$$N_{stream} = N_{POP} - N_{sr} \tag{13}$$

The stream population moving to sea and river can be expressed by

$$Population\ of\ streams = \begin{bmatrix} S_1 \\ S_2 \\ S_3 \\ . \\ . \\ S_{N_{stream}} \end{bmatrix} = \begin{bmatrix} A_1^1 & A_2^1 & A_3^1 & \ldots & A_N^1 \\ A_1^2 & A_2^2 & A_3^2 & \ldots & A_N^2 \\ . & . & . & . & . \\ . & . & . & . & . \\ A_1^{N_{stream}} & A_2^{N_{stream}} & A_3^{N_{stream}} & . & A_N^{N_{stream}} \end{bmatrix} \tag{14}$$

Now the number of streams moving to rivers and sea can be found as:

$$NS_n = round\left\{\left|\frac{C_n}{\sum_{n=1}^{N_{sr}} C_n}\right| \times N_{streams}\right\} \tag{15}$$

where $n = 1, 2, 3 \ldots.., N_{sr}$

$$C_n = Cost_n - Cost_{N_{sr+1}}, \quad n = 1, 2, 3 \ldots.., N_{sr} \tag{16}$$

N_{sr} is the count of streams, which moves to specified sea and rivers. Fig.5 represents the stream's flow to a specified river with the connection line.

The new positions of streams and rivers are proposed in the following equations:

$$\vec{A}_{stream}(t+1) = \vec{A}_{stream}(t) + rand \times, C\left(\vec{A}_{sea}(t) - \vec{A}_{stream}(t)\right) \tag{17}$$

$$\vec{A}_{stream}(t+1) = \vec{A}_{stream}(t) + rand \times, C\left(\vec{A}_{river}(t) - \vec{A}_{stream}(t)\right) \tag{18}$$

$$\vec{A}_{river}(t+1) = \vec{A}_{river}(t) + rand \times C\left(\vec{A}_{sea}(t) - \vec{A}_{river}(t)\right) \tag{19}$$

where t is marked as iteration index, and the rand is steadily distributed between zero and one. The updating equation (17) depicts the movement of the stream towards the sea, equation (18) represents the movement of the stream to the rivers. Equation (19) is representing the movement of rivers towards the sea. If the solution of any stream is superior to the connected river, then their positions are interchanged. So, the following iteration appraises stream as river and river as a stream. However, the same applies to a river and sea.

The next step is evaporation which results in precipitation. This step prevents premature convergence to local optima. For this river and streams should be in the neighborhood of sea. The equation (20) checks if evaporation followed by rain will occur in a river or stream

$$if \left\| \vec{A}^t_{sea} - \vec{A}^t_{river_j} \right\| < d_{max} orrand < 0.1 \quad Wherej = 1, 2, 3, \ldots.., N_{sr} - 1 \tag{20}$$

where d_{max} is very small and near zero, this value determines the search depth close to the sea. The higher value will increase the search intensity, whereas the smaller one decreases the search intensity.

The value of d_{max} decreases after each iteration as per the following equation.

$$d_{max}(t+1) = d_{max}(t) - \frac{d_{max}(t)}{Max.iteration} \quad Where\ t = 1, 2, 3, \ldots\ldots, Max.iteration. \tag{21}$$

Once evaporation activity is fulfilled, then the raining procedure is applied. The new raindrops from streams fall at distinct positions. The position on newly set up streams can be calculated using the equation below.

$$A^{new}_{stream} = LB + rand \times (UB - LB) \tag{22}$$

where UB is the upper bound and LB is the lower bound specified by the system. The flowchart of the WCA is shown in Fig.6.

As described above in this section, the sea or rivers, or streams are considered as raindrops by the WCA, and an array characterizes the raindrops. The sea is the finest raindrop, as it has the least objective function value (for depreciation). The water cycle algorithm tunes the parameters of PI and FOPI controllers. The problem variables in the VFOC scheme of the PWM rectifier are K_P, K_I for PI controller, whereas K_P, K_I, and λ for FOPI controllers. So, these variables are defined as stream (raindrops) arrays. The cost function is integral time absolute error (ITAE). The selected population size is 50. The LB is taken as zero, and UB is selected as 20. The value of d_{max} is taken as 1e-^{16}. The outer loop PI controller parameters obtained by WCA are K_P =0.4048 and K_I =20. The inner loop PI parameters obtained by WCA are K_P =0.2179, K_I =11.7736. The outer loop FOPI parameters obtained by WCA are K_P =0.3713, K_I =1.9075, and λ =1.0006. The inner loop FOPI parameters obtained by WCA are K_P =17.593, K_I =14.04, and λ =0.7942.

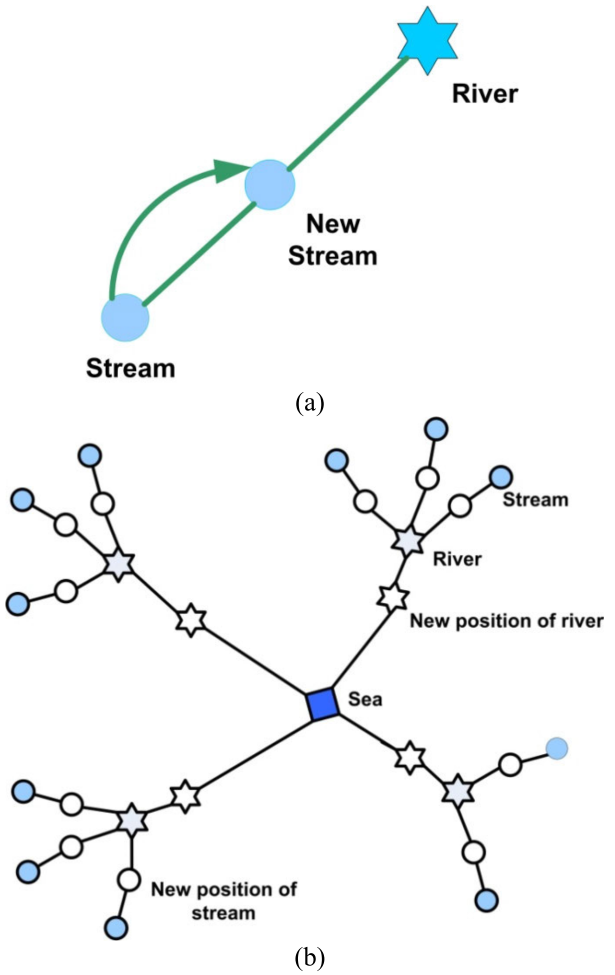

FIGURE 5. Schematic diagram showing (a) Flow of streams into a river; (b) WCA optimization procedure.

V. SIMULATION RESULTS

The proposed method of VFOC using WCA-PI and WCA-FOPI is verified using Matlab with Simulink and Fomcon toolbox. "The FOMCON toolbox for MATLAB is a fractional-order calculus-based toolbox for system modeling and control design. The approximation implemented in the toolbox is the most used Oustaloup Recursive Approximation (ORA)." The approximation order is set to 5, and the frequency range is taken as (0.001, 1000) for approximation. The simulation study is done under three conditions. In the first case, the simulation is performed with a three-phase balanced and ideal supply. In the second case, it is implemented with line filter parametric uncertainties. The value of line filter resistance and inductance is decreased. And in the third case, the performance of the rectifier is evaluated under unbalanced and distorted supply conditions.

A. PROPOSED VFOC SCHEME WITH BALANCED SUPPLY

The VFOC method using WCA-PI and WCA-FOPI controllers is simulated using MATLAB/Simulink. A three-grid supply line voltage of 415V is given to the input terminals of

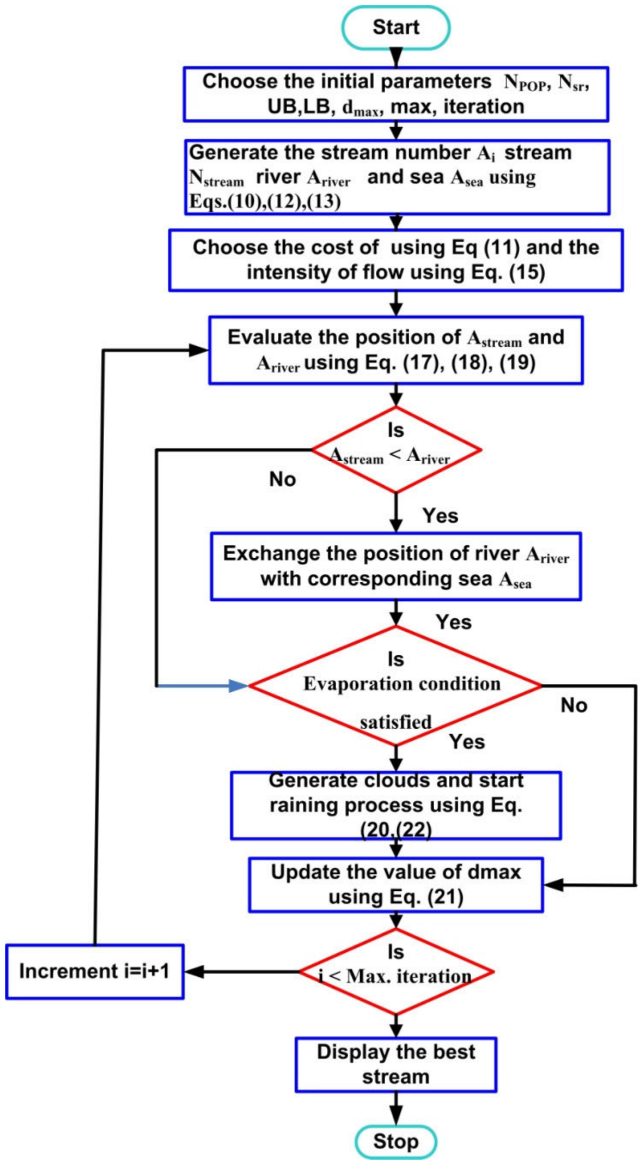

FIGURE 6. Flowchart of Water Cycle Algorithm.

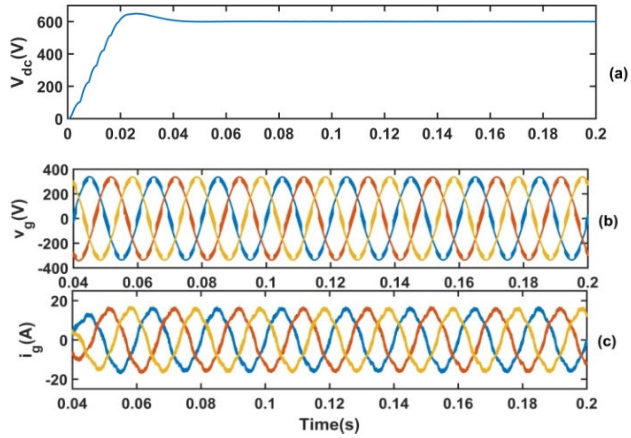

FIGURE 7. Performance of WCA-PI controller under balanced three phase supply (a) DC Link voltage three-phase voltage supply. (b) Three phase currents.

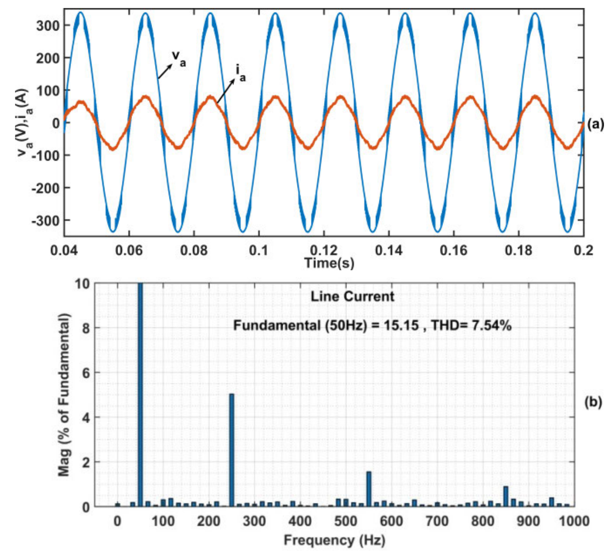

FIGURE 8. Phase a voltage and current at unity pf and frequency spectrum of line current generated by WCA-PI Under balanced three supply.

the rectifier, and dc reference voltage is set to 600V. The line filter parameters are 0.001Ω and 3 mH. A full resistive load of 10kW is connected across the capacitor. The simulation results using the WCA-PI controller are shown in Fig. 7-8.

The current scale is zoomed in five times to improve the visibility in Fig.8 (a). These figures demonstrate that the dc side voltage is 600V, the power factor is close to unity, and the THD of the supply phase current is 7.54%.

The simulation results using WCA-FOPI are shown in Fig. 9-10. The current scale is zoomed in five times to improve the visibility in Fig.10 (a). These figures demonstrate that the dc side voltage is 600V, the power factor is close to unity, and the THD of grid phase current is 1.49%.

Fig. 11 shows the comparison dc-link voltage of WCA-PI and WCA-FOPI controllers. It can be observed that the settling time of the FOPI controller is less than the PI controller, so the FOPI controller improved the stability of the system. The peak overshoot is 660V using the WCA-PI controller and 600 V using the WCA-FOPI controller. The rise time is 0.02-sec using WCA-FOPI and using 0.042 using the WCA-PI controller. The THD of phase current is 7.54% with WCA-PI and 1.49% with WCA-FOPI controller. The FOPID controller provides better control of the non-linear system, resulting in less current harmonics with WCA-FOPI than the WCA-PI controller. It can be concluded that the control action in terms of rise time, peak-overshoot and harmonic content is better using WCA-FOPI controller. The Fig.12 shows the convergence characteristics of WCA-PI and WCA-FOPI controllers. This figure demonstrates that the WCA-FOPI converges faster than WCA-PI.

A step change in load is applied at from 10kW to 15 kW at 0.1 sec and then from 15kW to 20 kW at 0.15 sec. The load

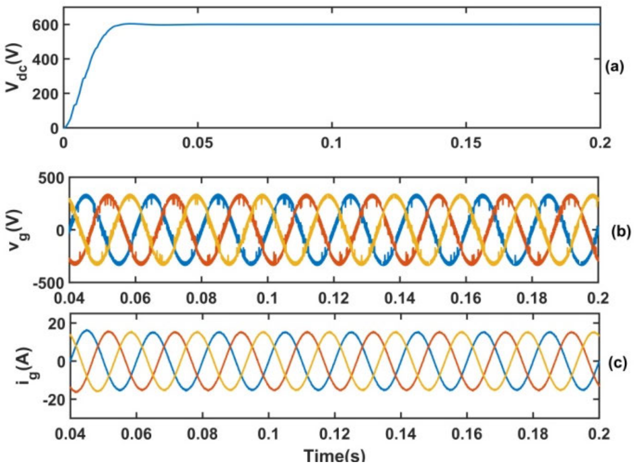

FIGURE 9. Performance of WCA-FOPI controller under balanced three-phase supply (a) DC Link voltage three-phase voltage supply. (b) Three-phase currents.

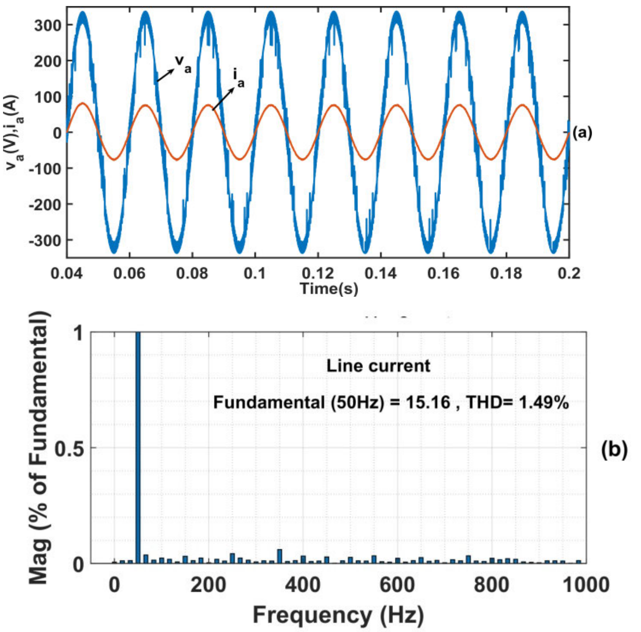

FIGURE 10. Phase a voltage and current at unity pf and frequency spectrum of line current generated by WCA-FOPI under balanced three supply.

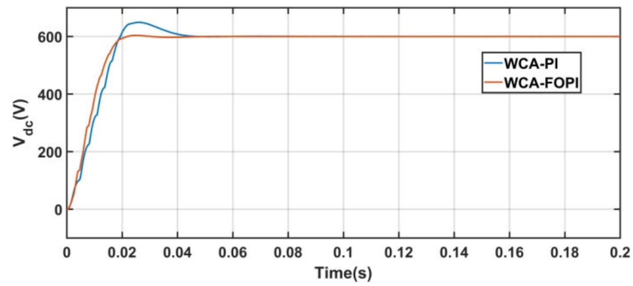

FIGURE 11. The DC link voltage using WCA-PI and WCA-FOPI controllers under balanced three phase supply.

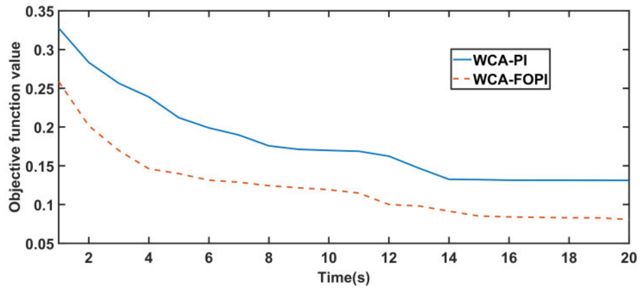

FIGURE 12. Convergence characteristics of WCA-PI and WCA-FOPI.

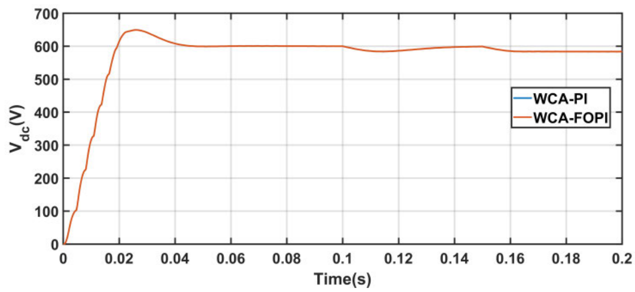

FIGURE 13. Load disturbance characteristics of WCA-PI and WCA-FOPI.

disturbance characteristics of output voltage are overlapped in the both cases as shown in Fig.13 It is observed that both WCA-PI and WCA-FOPI provide same type of behavior under load disturbances. The load voltage is restored to reference voltage when load is increased to 15 kW. But when the load is increased to 20 kW, the load voltage does not reach set point using WCA-PI and WCA-FOPI. The Fig.14 shows the effect of controller saturation on the output dc voltage. A step change in reference voltage is applied at 0.1 sec from 600V to 700V. The output response in WCA-PI is delayed more than WCA-FOPI controller. The output voltage settles to reference voltage of 700V at 0.14 sec with WCA-FOPI and at 0.18 sec in the WCA-PI controller. The Fig.15 shows the reference sine waveform for generating PWM. The noise present in the modulating waveform of WCA-PI and WCA-FOPI is reflected into the response of the rectifier. The output of WCA-PI and WCA-FOPI controller of inner control loop is shown in Fig.16 and Fig.17 respectively. The bode plot of outer voltage loop is given in Fig.18.The gain margins are 48.908dB and 44.5278 dB using WCA-FOPI and WCA-PI controllers, respectively. The phase margin with WCA-FOPI controller is 110.14 and 98.01 using WCA-PI controller. The WCA-FOPI has more gain and phase margin compared to WCA-PI controller.

B. PROPOSED VFOC SCHEME UNDER PARAMETRIC UNCERTAINTIES

The VFOC method using both types of controllers under parametric variation is simulated using MATLAB/Simulink. A three-grid line voltage of 415V is voltage is set to 600V. The line filter parameters are reduced to 0.0008Ω and 2.8 mH.

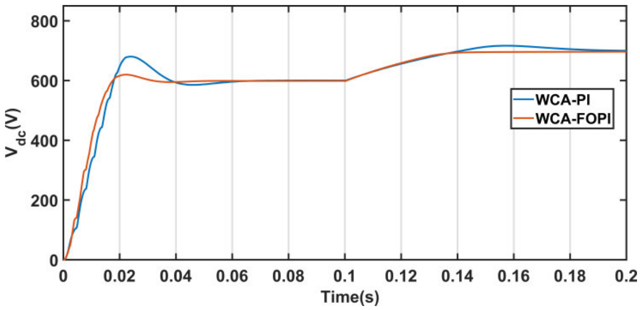

FIGURE 14. The controller undersaturation in WCA-PI and WCA-FOPI.

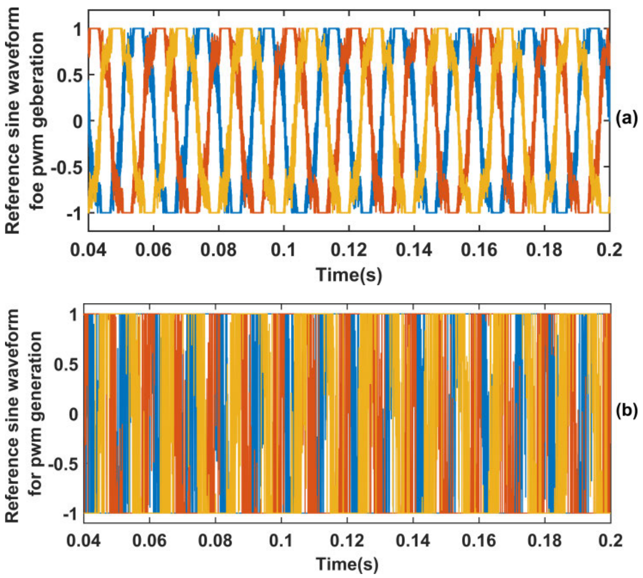

FIGURE 15. Reference sine waveform for PWM signal generation for (a) WCA-PI (b) WCA-FOPI.

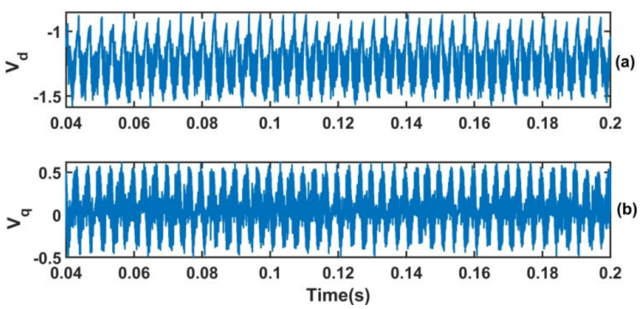

FIGURE 16. The output of the inner loop WCA-PI controller.

The filter inductor parameters are changed uniformly in all three phases. A full resistive load of 10kW is connected. The simulation results are shown in Fig. 19-21. The current scale is zoomed in five times to improve the visibility in Fig.20 (a) and Fig. 21(a). The comparison of dc voltage tracking using both types of controllers are shown in Fig.17.The peak overshoot using WCA-PI is more than using the WCA-FOPI controller. The rise time is shorter with WCA-FOPI than WCA-PI controller. The power factor close to unity is

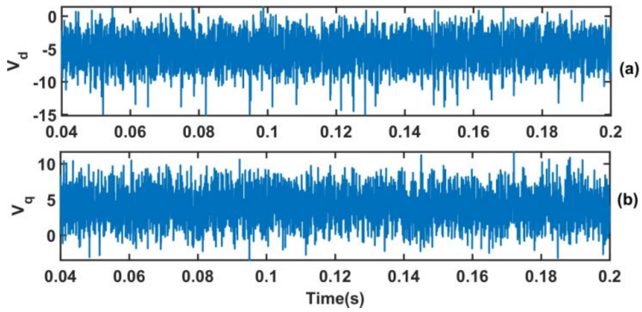

FIGURE 17. The output of the inner loop WCA-FOPI controller.

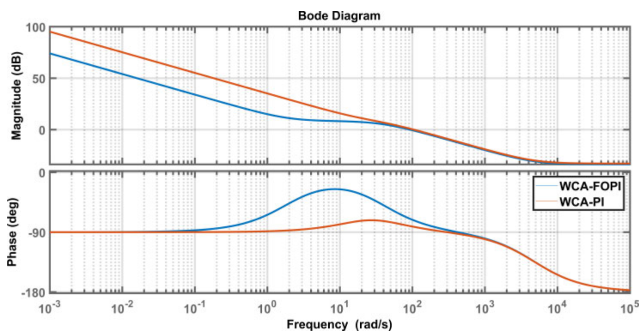

FIGURE 18. Bode plot of the outer voltage loop with WCA-PI and WCA-FOPI.

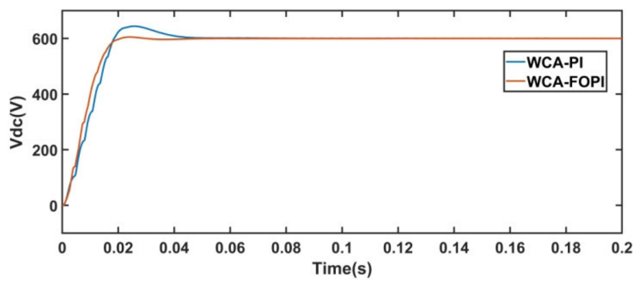

FIGURE 19. The DC link voltage using WCA-PI and WCA-FOPI controllers under parametric uncertainties.

achieved using both types of controllers. Moreover, the THD using WCA-PI controller is increased to 8.44%, and using WCA-PI controller is 1.59%. So, it is concluded that the WCA-FOPI controller provides a better control effect than the WCA-PI controller under parametric variations. It can be summarized that WCA-FOPI provides more robustness against parametric uncertainties.

C. PROPOSED VFOC SCHEME USING FOPI UNDER UNBALANCE AND DISTORTED SUPPLY

The VFOC method using both types of controllers under unbalance supply voltage is simulated using MATLAB/Simulink. A three-grid line voltage of 415V is given to the input terminals of the rectifier, and dc reference voltage is set to 600V. The line filter parameters are 0.001Ω and 3 mH. A full resistive load of 10kW is connected across the capacitor. The simulation results can be seen in Fig. 22-25.

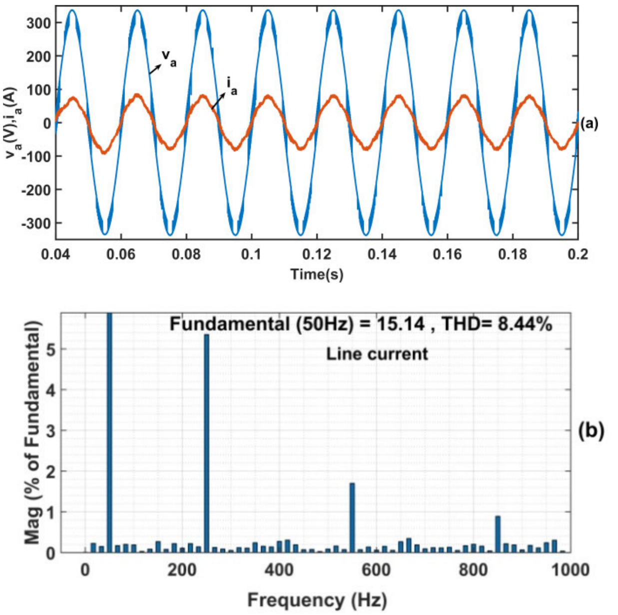

FIGURE 20. Phase a voltage and current at unity pf and frequency spectrum of line current generated by WCA-PI under parametric variations.

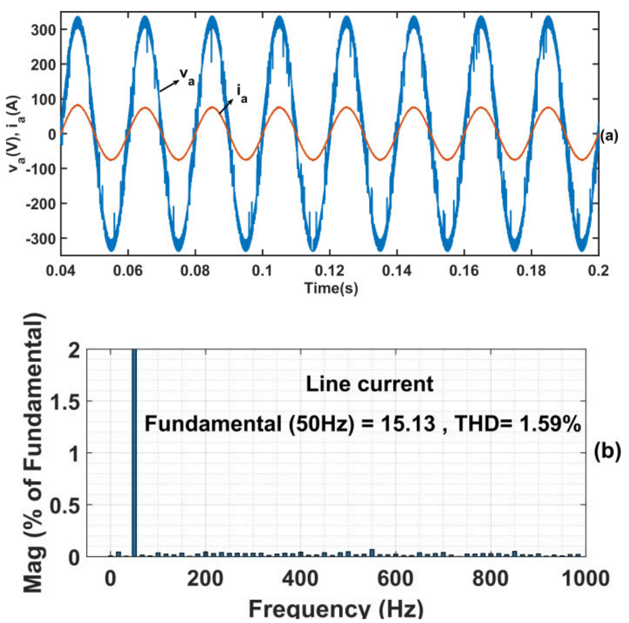

FIGURE 21. (a) Phase a voltage and current at unity pf and (b) Frequency spectrum of line current generated by WCA-FOPI under parametric variations.

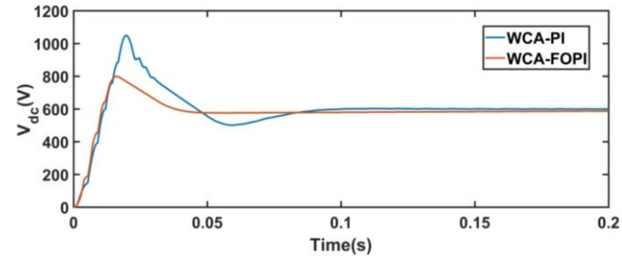

FIGURE 22. The DC link voltage using WCA-PI and WCA-FOPI controllers under unbalanced and distorted three-phase supply.

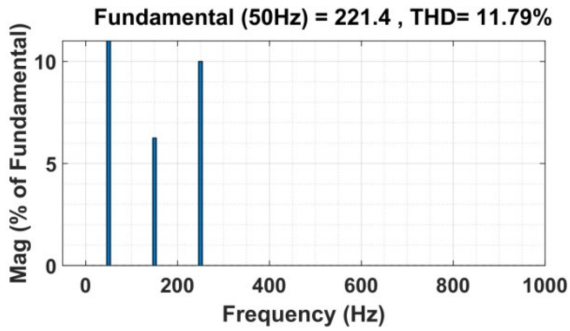

FIGURE 23. The frequency spectrum of phase a supply voltage.

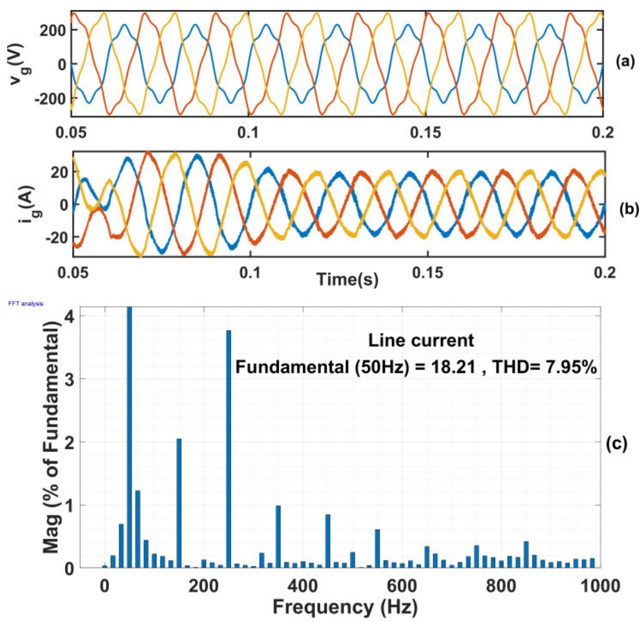

FIGURE 24. Three-phase voltage and current at unity pf and frequency spectrum of line current generated by WCA-PI under unbalanced and distorted three-phase supply.

The unbalance is due to different voltages of three phases. The THD of phase a supply voltage is 11.79%, as shown in Fig.23.

The comparison of dc voltage tracking using both types of controllers are shown in Fig.22. The peak overshoot using WCA-PI is 1050V and 800 V using the WCA-FOPI controller. The settling time is shorter with WCA-FOPI than with the WCA-PI controller. The power factor close to unity is achieved using both types of controllers. Moreover, the THD using WCA-PI controller is increased to 7.95%, and using WCA-PI controller is 1.63%. However, both types of controllers draw balanced supply current during unbalanced and distorted supply conditions. It can be validated that

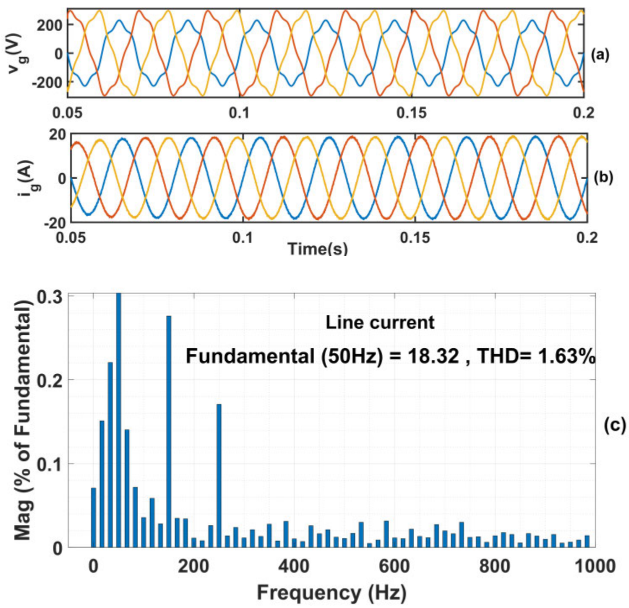

FIGURE 25. Three phase voltage and current at unity pf and frequency spectrum of line current generated by WCA-FOPI under unbalanced and distorted three-phase supply.

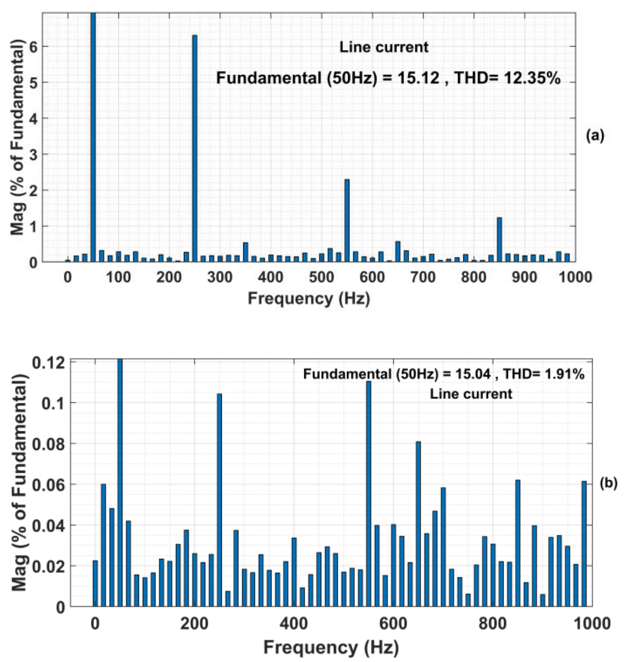

FIGURE 26. The frequency spectrum of line current with line filter inductance L=2.2 mH (a) WCA-PI (b) WCA-FOPI.

WCA-FOPI demonstrates more robustness against supply disturbances

A comparison of THD and peak overshoot obtained by using both type controllers under different conditions is made in table 1. It can be concluded from the table that the WCA-FOPI controller provides more robustness and better control effect than the WCA-PI controller.

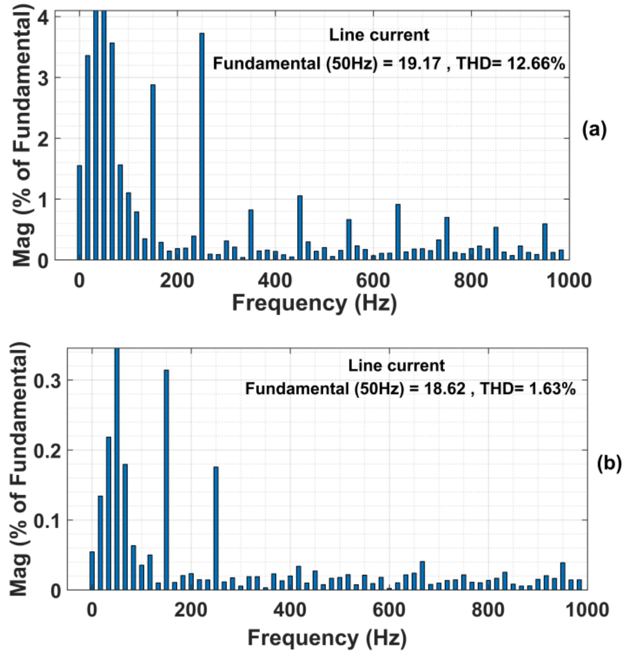

FIGURE 27. The frequency spectrum of line current with phase a voltage reduced by 25% (a) WCA-PI (b) WCA-FOPI.

TABLE 1. Comparison of THD and Peak overshoot.

Control effect	WCA-PI	WCA-FOPI
THD under ideal supply	7.54%	1.49%
THD under parametric uncertainties	8.44%	1.59%
THD under Non-ideal supply voltage	7.95%	1.63%
Peak-overshoot under ideal supply	660V	600V
Peak-overshoot under Parametric uncertainties	650V	600V
Peak-overshoot under Non-ideal supply voltage	1050V	800V

D. SENSITIVITY ANALYSIS

Considering the base case of balanced supply conditions in section V(A), a sensitivity analysis is carried out to prospect the effectiveness of the proposed controller with a -26.67% change in line filter inductance value, 25% voltage sag in phase a to create unbalance. The results are shown in Fig.26-27.

The value of the inductance of the line filter is reduced by 26.67% (2.2 mH) compared to the base case. The THD of grid current is increased to 12.35 % and 1.91% with WCA-PI and WCA-FOPI, respectively. For a change of the line filter value by -26.67%, the THD of grid current increased by 63.79% for WCA-PI and 28.18% for WCA-FOPI controllers. The FOPI controller is less sensitive to parametric variation of line filters. The voltage of phase a is reduced by 25% compared to the base case, and the other phase's voltage is kept to a normal value. The line current THD increased to 12.66%

and 1.63% for WCA-PI and WCA-FOPI, respectively. For a change in the input voltage of 25%, the THD of grid current changes by 67.9% for the WCA-PI controller and 2.515% for the WCA-FOPI controller. Therefore, the WCA-FOPI is less sensitive to input voltage variations. It can be concluded that the WCA-FOPID controller is more robust to parametric variations and supply disturbances.

VI. CONCLUSION

A water cycle algorithm-based fractional order PI controller is proposed to implement a virtual flux-oriented control scheme in a three-phase PWM rectifier. Water cycle-based fractional-order PI (WCA-PI) and integer-order PI (WCA-PI) controllers are designed and optimized. WCA is an optimization method inspired by monitoring the water cycle operation and flow of water bodies like streams and rivers toward the sea. The fractional-order controllers have an additional degree of freedom and provide a more robust control effect. The major benefit of the FOPID controller is to increase the performance of non-linear and dynamic systems; have less sensitivity to changes in parameters of the system. The rectifier is operated under three conditions: a) balanced supply conditions, b) parametric uncertainties, c) unbalance and distorted supply conditions. The simulation results verify the better performance of WCA-FOPI in terms of settling time and stability, rise time, peak overshoot, and Total Harmonic distortion of grid current under balance supply conditions. The WCA-FOPI converges faster than WCA-PI. Both types of controllers observed the same response under load disturbances. The input line filter parameters are changed to evaluate the performance under parametric uncertainties. The value of inductance and resistance is reduced. A more robust response is recorded with WCA-FOPI.

Moreover, under unbalance and distorted supply, both types of controllers give balanced supply currents. However, the peak overshoot, settling time, and THD of grid current are increased under unbalance and distorted supply voltage. But the WCA-FOPI is found to be better and more robust in these evaluation parameters. The simulation findings validate the WCA-FOPI controller outcomes as compared to WCA-PI in terms of control effect and robustness.

ACKNOWLEDGMENT

The authors are thankful to the Department of Electrical Engineering, Indian Institute of Technology (Indian School of Mines), Dhanbad, India, for providing necessary laboratory facilities to complete this research work in its present shape. The first author would like to acknowledge Dr. R. K. Saket of the Department of Electrical Engineering, Indian Institute of Technology (BHU), Varanasi, Uttar Pradesh, India, for his encouragements and technical suggestions to complete this research work smoothly.

REFERENCES

[1] M. Malinowski, M. Jasinski, and M. P. Kazmierkowski, "Simple direct power control of three-phase PWM rectifier using space-vector modulation (DPC-SVM)," *IEEE Trans. Ind. Electron.*, vol. 51, no. 2, pp. 447–454, Apr. 2004.

[2] T. Noguchi, H. Tomiki, S. Kondo, and I. Takahashi, "Direct power control of PWM converter without power-source voltage sensors," *IEEE Trans. Ind. Appl.*, vol. 34, no. 3, pp. 473–479, May/Jun. 1998.

[3] M. Malinowski, M. P. Kazmierkowski, and A. Trzynadlowski, "Review and comparative study of control techniques for three-phase PWM rectifiers," *Math. Comput. Simul.*, vol. 63, nos. 3–5, pp. 349–361, Nov. 2003.

[4] M. Malinowski, "Adaptive space vector modulation for three-phase two-level PWM rectifiers/inverters," *Arch. Electr. Eng.*, vol. 1, no. 3, pp. 281–295, 2002.

[5] K. J. Astrom and T. Hagglund, *PID Controllers: Theory, Design and Tuning*. Research Triangle, NC, USA: Instrument Society of America, 1995.

[6] A. Tepljakov, B. B. Alagoz, C. Yeroglu, E. Gonzalez, S. H. HosseinNia, and E. Petlenkov, "FOPID controllers and their industrial applications," *IFAC-Papers OnLine*, vol. 51, no. 4, pp. 25–30, 2018.

[7] A. Tepljakov, B. B. Alagoz, C. Yeroglu, E. A. Gonzalez, S. H. Hosseinnia, E. Petlenkov, A. Ates, and M. Cech, "Towards industrialization of FOPID controllers: A survey on milestones of fractional-order control and pathways for future developments," *IEEE Access*, vol. 9, pp. 21016–21042, 2021.

[8] O. Gül and N. Tan, "Application of fractional-order voltage controller in building-integrated photovoltaic and wind turbine system," *Meas. Control*, vol. 52, nos. 7–8, pp. 1145–1158, Jul. 2019.

[9] M. Lakshmi and S. Hemamalini, "Decoupled control of grid connected photovoltaic system using fractional order controller," *Ain Shams Eng. J.*, vol. 9, no. 4, pp. 927–937, Dec. 2018.

[10] A. Mughees and S. A. Mohsin, "Design and control of magnetic levitation system by optimizing fractional order PID controller using ant colony optimization algorithm," *IEEE Access*, vol. 8, pp. 116704–116723, 2020.

[11] A. K. Mishra, S. R. Das, P. K. Ray, R. K. Mallick, A. Mohanty, and D. K. Mishra, "PSO-GWO optimized fractional order PID based hybrid shunt active power filter for power quality improvements," *IEEE Access*, vol. 8, pp. 74497–74512, 2020.

[12] S.-W. Seo and H. H. Choi, "Digital implementation of fractional order PID-type controller for boost DC–DC converter," *IEEE Access*, vol. 7, pp. 142652–142662, 2019.

[13] C.-H. Hsu, "Fractional order PID control for reduction of vibration and noise on induction motor," *IEEE Trans. Magn.*, vol. 55, no. 11, pp. 1–7, Nov. 2019.

[14] Y. Arya, "A novel CFFOPI-FOPID controller for AGC performance enhancement of single and multi-area electric power systems," *ISA Trans.*, vol. 100, pp. 126–135, May 2020.

[15] M. S. Ayas and E. Sahin, "FOPID controller with fractional filter for an automatic voltage regulator," *Comput. Electr. Engg.*, vol. 90, pp. 1–11, Mar. 2021.

[16] Z. Bingul and O. Karahan, "A novel performance criterion approach to optimum design of PID controller using cuckoo search algorithm for AVR system," *J. Franklin Inst. B*, vol. 355, no. 13, pp. 5359–5534, 2018.

[17] S. Ekinci and B. Hekimoglu, "Improved kidney-inspired algorithm approach for tuning of PID controller in AVR system," *IEEE Access*, vol. 7, pp. 39935–39947, 2019.

[18] Y. Tang, M. Cui, C. Hua, L. Li, and Y. Yang, "Optimum design of fractional order $PI^{\lambda}D^{\mu}$ controller for AVR system using chaotic ant swarm," *Expert Syst. Appl.*, vol. 39, no. 8, pp. 6887–6896, Jun. 2012.

[19] G.-Q. Zeng, J. Chen, Y.-X. Dai, L.-M. Li, C.-W. Zheng, and M.-R. Chen, "Design of fractional order PID controller for automatic regulator voltage system based on multi-objective extremal optimization," *Neurocomputing*, vol. 160, pp. 173–184, Jul. 2015.

[20] R. Lahcene, S. Abdeldjalil, and K. Aissa, "Optimal tuning of fractional order PID controller for AVR system using simulated annealing optimization algorithm," in *Proc. Int. Conf. Electr. Eng., Boumerdes*, Oct. 2017, pp. 1–6.

[21] G. Tzounas, I. Dassios, M. A. A. Murad, and F. Milano, "Theory and implementation of fractional order controllers for power system applications," *IEEE Trans. Power Syst.*, vol. 35, no. 6, pp. 4622–4631, Nov. 2020.

[22] A. Bensenouci and M. Shehata, "Optimized FOPID control of a single link flexible manipulator (SLFM) using genetic algorithm," *Appl. Mech. Mater.*, vol. 704, pp. 336–340, Dec. 2014.

[23] M. A. Shamseldin, A. A. EL-Samahy, and A. M. A. Ghany, ''Different techniques of self-tuning FOPID control for brushless DC motor,'' in *Proc. Int. Middle East Power Syst. Conf. (MEPCON)*, Cairo, Egypt, Dec. 2016, pp. 342–347.

[24] M. S. Gaballa, M. Bahgat, and A.-G.-M. Abdel-Ghany, ''A novel technique for online self-tuning of fractional order PID, based on Takaji–Sugeno fuzzy,'' in *Proc. 19th Int. Middle East Power Syst. Conf. (MEPCON)*. Shebeen El-Kom, Egypt: Menoufia Univ., Dec. 2017, pp. 19–21.

[25] S. G. Samko, A. A. Kilbas, and O. I. Marichev, *Fractional Integrals and Derivatives and Some of Their Applications*. New York, NY, USA: Gordon and Breach, 1993.

[26] D. Xue and Y. Q. Chen, *MATLAB Solutions to Advanced Applied Mathematical Problems*. Beijing, China: Tsinghua Univ. Press, 2004.

[27] H. O. Erkol, ''Optimal $PI^{\lambda}D^{\mu}$ controller design for two wheeled inverted pendulum controller design for two wheeled inverted pendulum,'' *IEEE Access*, vol. 6, pp. 75709–75717, 2018.

[28] X. Li, Y. Wang, N. Li, M. Han, Y. Tang, and F. Liu, ''Optimal fractional order PID controller design for automatic voltage regulator system based on reference model using particle swarm optimization,'' *Int. J. Mach. Learn. Cybern.*, vol. 8, no. 5, pp. 1595–1605, 2017.

[29] V. H. Haji and C. A. Monje, ''Fractional order fuzzy-PID control of a combined cycle power plant using particle swarm optimization algorithm with an improved dynamic parameters selection,'' *Appl. Soft Comput.*, vol. 58, pp. 256–264, Sep. 2017.

[30] J. Fang, ''The LQR controller design of two-wheeled self-balancing robot based on the particle swarm optimization algorithm,'' *Math. Problems Eng.*, vol. 2014, pp. 1–6, May 2014.

[31] A. X. R. Irudayaraj, N. I. A. Wahab, M. G. Umamaheswari, M. A. M. Radzi, N. B. Sulaiman, V. Veerasamy, S. C. Prasanna, and R. Ramachandran, ''A Matignon's theorem based stability analysis of hybrid power system for automatic load frequency control using atom search optimized FOPID controller,'' *IEEE Access*, vol. 8, pp. 168751–168772, 2020.

[32] B. Hekimoğlu, ''Optimal tuning of fractional order PID controller for DC motor speed control via chaotic atom search optimization algorithm,'' *IEEE Access*, vol. 7, pp. 38100–38114, 2019.

[33] A. Ateş and C. Yeroglu, ''Optimal fractional order PID design via Tabu search based algorithm,'' *ISA Trans.*, vol. 60, pp. 109–118, Jan. 2016.

[34] T. Mahto and V. Mukherjee, ''Fractional order fuzzy PID controller for wind energy-based hybrid power system using quasi-oppositional harmony search algorithm,'' *IET Gener., Transmiss. Distrib.*, vol. 11, no. 13, pp. 3299–3309, Sep. 2017.

[35] S. K. Verma, S. Yadav, and S. K. Nagar, ''Optimization of fractional order PID controller using grey wolf optimizer,'' *J. Control, Autom. Electr. Syst.*, vol. 28, no. 3, pp. 314–322, Jun. 2017.

[36] L. Lu, S. Liang, D. Yuewei, L. Chenglin, and Q. Zhidong, ''Improved quantum bacterial foraging algorithm for tuning parameters of fractional-order PID controller,'' *J. Syst. Eng. Electron.*, vol. 29, no. 1, pp. 166–175, 2018.

SUSHMA KAKKAR received the B.Tech. degree in electrical engineering from the National Institute of Technology, Kurukshetra, India, and the M.Tech. degree in power electronics, electric machines and drives from the Indian Institute of Technology, New Delhi, India. She is currently pursuing the Ph.D. degree in electrical engineering with the Indian Institute of Technology (Indian School of Mines), Dhanbad, India. Her research interests include power electronics, power quality, and distributed generation.

TANMOY MAITY (Member, IEEE) received the master's degree in electrical engineering from Calcutta University, Kolkata, India, and the Ph.D. degree from Bengal Engineering and Science University, Shibpur, India. He has six years of industrial and more than 18 years of academic experience. He is currently working as an Associate Professor with the Indian Institute of Technology (ISM), Dhanbad, Jharkhand, India. His research interests include power electronics, power quality, power systems, and distributed generation.

RAJESH KUMAR AHUJA (Member, IEEE) received the B.E. degree from Nagpur University, the M.Tech. degree from the Indian Institute of Technology, Kharagpur, India, and the Ph.D. degree from the Indian Institute of Technology, New Delhi, India. He has more than two decades of teaching and research experience. He is currently working as a Professor with J. C. Bose YMCA University of Science and Technology, Faridabad, Haryana, India. His research interests include renewable energy, induction generators, power electronics, electrical machines, and drives.

PRATIMA WALDE received the B.E. degree in electrical engineering from Government Engineering College, Jabalpur, Madhya Pradesh, India, in 1998, the M.E. degree from MITS, Gwalior, Madhya Pradesh, in 2003, and the Ph.D. degree from the Indian Institute of Technology (BHU), in 2009. From January 2003 to April 2008, she worked as a Senior Research Fellow with the Department of Electrical Engineering, Banaras Hindu University, Varanasi, India. Her research interests include deregulation, optimization, and AI application to power systems.

R. K. SAKET (Senior Member, IEEE) was a Faculty Member with Birla Institute of Technology and Science, Pilani, Rajasthan, India; the University Institute of Technology, Rajiv Gandhi University of Technology, Bhopal, Madhya Pradesh, India; and Sam Higginbottom University of Agriculture, Technology and Sciences, Allahabad, Uttar Pradesh, India. He is currently a Professor with the Department of Electrical Engineering, Indian Institute of Technology (Banaras Hindu University), Varanasi, India. He has more than 20 years of academic and research experience. He is the author/coauthor of approximately 140 scientific articles, book chapters, and research papers in indexed international journals and prestigious conference proceedings. He is a fellow of the Institution of Engineers, India; a member of IET, U.K., and a Life Member of the Indian Society for Technical Education, New Delhi, India. He is an Associate Editor of the *IET Renewable Power Generation*, U.K.; and IEEE Access, USA. He is an Editorial Board Member of the *Journal of Electrical Systems*, France, and *Engineering, Technology and Applied Science Research*, Greece. He has received many awards, honors, and recognitions for his academic and research contributions, including the prestigious Gandhian Young Technological Innovation Award–2018 appreciated by the Hon'ble President of India at Rashtrapati Bhavan, New Delhi, India, Design Impact Award–2018 appreciated by Padma Vibhushan Ratan Tata at Mumbai, India, and Nehru Encouragement Award—1988 and 1990 awarded by the Hon'ble Chief Minister of Madhya Pradesh State Government, Bhopal, India.

BASEEM KHAN (Member, IEEE) received the B.Eng. degree in electrical engineering from Rajiv Gandhi Technological University, Bhopal, India, in 2008, and the M.Tech. and D.Phil. degrees in electrical engineering from Maulana Azad National Institute of Technology, Bhopal, in 2010 and 2014, respectively. He is currently working as a Faculty Member with Hawassa University, Ethiopia. His research interests include power system restructuring, power system planning, smart grid technologies, meta-heuristic optimization techniques, reliability analysis of renewable energy systems, power quality analysis, and renewable energy integration.

SANJEEVIKUMAR PADMANABAN (Senior Member, IEEE) received the Ph.D. degree in electrical engineering from the University of Bologna, Bologna, Italy, in 2012.

He was an Associate Professor with VIT University from 2012 to 2013. In 2013, he joined the National Institute of Technology, India, as a Faculty Member. In 2014, he was invited as a Visiting Researcher with the Department of Electrical Engineering, Qatar University, Doha, Qatar, funded by the Qatar National Research Foundation (Government of Qatar). He continued his research activities with the Dublin Institute of Technology, Dublin, Ireland, in 2014. He served as an Associate Professor for the Department of Electrical and Electronics Engineering, University of Johannesburg, Johannesburg, South Africa, from 2016 to 2018. From March 2018 to February 2021, he has been a Faculty Member with the Department of Energy Technology, Aalborg University, Esbjerg, Denmark. Since March 2021, he has been with the CTIF Global Capsule (CGC) Laboratory, Department of Business Development and Technology, Aarhus University, Herning, Denmark. He has authored over 300 scientific articles. He is a fellow of the Institution of Engineers, India, the Institution of Electronics and Telecommunication Engineers, India, and the Institution of Engineering and Technology, U.K. He was a recipient of the Best Paper cum Most Excellence Research Paper Award from IET-SEISCON'13, IET-CEAT'16, IEEE-EECSI'19, IEEE-CENCON'19, and five best paper awards from ETAEERE'16 sponsored Lecture Notes in Electrical Engineering, Springer book. He is an Editor/Associate Editor/Editorial Board for refereed journals, in particular the IEEE Systems Journal, IEEE Transaction on Industry Applications, IEEE Access, *IET Power Electronics*, *IET Electronics Letters*, and *International Transactions on Electrical Energy Systems* (Wiley), a Subject Editorial Board Member of *Energy Sources, Energies* journal (MDPI), and a Subject Editor of the *IET Renewable Power Generation*, *IET Generation*, *Transmission and Distribution*, and *FACETS* journal, Canada.